

# Generative Face Parsing Map Guided 3D Face Reconstruction Under Occluded Scenes

Dapeng Zhao<sup>1</sup> and Yue Qi<sup>1,2,3</sup>

<sup>1</sup> State Key Laboratory of Virtual Reality Technology and Systems, School of Computer Science and Engineering at Beihang University, Beijing, China  
mirror1775@gmail.com

<sup>2</sup> Peng Cheng Laboratory, Shenzhen, China

<sup>3</sup> Qingdao Research Institute of Beihang University, Qingdao, China

**Abstract.** Over the past few years, single-view 3D face reconstruction methods can produce beautiful 3D models. Nevertheless, the input of these works is unobstructed faces. We describe a system designed to reconstruct convincing face texture in the case of occlusion. Motivated by parsing facial features, we propose a complete face parsing map generation method guided by landmarks. We estimate the 2D face structure of the reasonable position of the occlusion area, which is used for the construction of 3D texture. An excellent anti-occlusion face reconstruction method should ensure the authenticity of the output, including the topological structure between the eyes, nose, and mouth. We extensively tested our method and its components, qualitatively demonstrating the rationality of our estimated facial structure. We conduct extensive experiments on general 3D face reconstruction tasks as concrete examples to demonstrate the method's superior regulation ability over existing methods often break down. We further provide numerous quantitative examples showing that our method advances both the quality and the robustness of 3D face reconstruction under occlusion scenes.

**Keywords:** 3D Face Reconstruction · Face Parsing · Occluded Scenes.

## 1 Introduction

3D face reconstruction refers to synthesizing a 3D face model given one input face photo. It has a wide range of applications, such as face recognition and digital entertainment [64]. Existing methods mainly concentrate on unobstructed faces, thus limiting the scenarios of their actual applications. Reconstructing a 3D face model from a single photo is a classical and fundamental problem in computer vision. The reconstruction task is challenging as human face structure partial invisibility when considering occluded scenes. Over the past five years, the related problem of face inpainting in images has gradually developed to the rationality of face photo generation in the most extreme scenes [45].

We cannot use artificial intelligence to robustly predict the 3D texture of the occluded area of the face. On the other hand, when faces are partially occluded, existing methods often indiscriminately reconstruct the occluded area. With the assistance of face parsing map, we find a way to identify the occluded area and reconstruct the input image to a reasonable 3D face model. The main contributions are summarized as follows:

- We propose a novel algorithm that combines feature points and face parsing map to generate face with complete facial features.
- To address the problem of invisible face area under occluded scenes, we propose synthesizing input face photo based on Generative Adversarial Network rather than reconstructing 3D face directly.
- We have improved the loss function of our 3D reconstruction framework for occluded scenes. Our method obtains state-of-the-art qualitative performance in real-world images.

## 2 Related Works

### 2.1 Generic Face Reconstruction

The classic methods use reference 3D face models to fit the input face photo. Some recent techniques use Convolution Neural Networks (CNNs) to regress landmark locations with the raw face image. Some recent techniques firstly used CNNs to predict the 3DMM parameters with input face image. Some works proposed a cascaded CNN structure to regress the accurate 3DMM shape parameters [26, 35, 49, 50, 76]. Some frameworks explored the end-to-end CNN architectures to regress 3DMM coefficients directly. Each calculation usually takes a long time because the dimensionality of the data is very high [14].

### 2.2 Face Parsing

A face parsing map generally serves as an intermediate representation for conditional face image generation [60]. In addition, the image-to-image GAN model can learn the mapping from the semantic map to realistic RGB image [23, 43, 44, 65][32-35]. In the pixel-level image semantic segmentation methods based on deep learning, FCN [38] is the well-known baseline for generic images which analyze per-pixel feature. Following this work, the DeepLab approaches [4, 5, 6, 7] have achieved impressive results. The main feature of the series is to use hole convolution instead of traditional convolution. However, directly applying these frameworks for face parsing may fail to map the varying-yet-concentrated facial features, especially hair, leading to poor results. A workable solution should directly predict per-pixel semantic label across the entire face photo. Wei et al. [66] proposed a novel method for regulating receptive fields with superior regulation ability in parsing networks to access accurate parsing map. MaskGan [29] contributed a labeled face dataset [37]. Zhou et al. [72] proposed an architecture that explored how to combine the fully-convolutional network model and super-pixel data to model together. In order to solve the question of global image

information access restriction, some methods [9, 34, 59, 68] have introduced the transformer component and achieved state-of-the-art results. The semantic layout guides the location and appearance of facial features and further facilitates the training. The majority of face parsing methods work require semantic labels. Hence, these frameworks [8, 19, 29, 31, 33, 55, 67] usually train on the CelebA and Helen dataset which contain labeled attributes.

### 2.3 Generative Adversarial Networks

Generative Adversarial Network (GAN) [16] generally consists of a generator and a discriminator. The two components compete with each other. Since GANs can generate realistic images, GANs have been successfully applied to various face image synthesis tasks, such as image manipulation [1, 24, 29, 73], image-to-image translation [23, 36, 44, 65, 74], image inpainting [10, 69] and texture blend [15, 30, 57]. For example, the face images generated by Stylegan2 [28] can reach a high degree of recognition. With continuous improvements in regularization [13, 22, 40, 44, 48, 63, 75], users can control the synthesis by feeding the generator with conditioning information instead of noise. Our work was built on conditional GANs [39] with face parsing map inputs, which aims to tackle face reconstruction under occluded scenes.

### 2.4 Face Image Synthesis

Deep pixel-level face generating has been studied for a few years. Many methods achieve remarkable results. Context encoder [46] is the first deep learning network designed for image inpainting with encoder-decoder architecture. Nevertheless, the networks do a poor job in dealing with human faces. Following this work, Yang et al. [65] used a modified VGG network [56] to improve the result of the context-encoder, by minimizing the feature difference of photo background. Dolhansky et al. [12] demonstrated the significance of exemplar data for inpainting. However, this method only focuses on filling in missing eye regions of the frontal face, so it does not generalize well. EdgeConnect [41] shows impressive proceeds which disentangling generation into two stages: edge generator and image completion network. Contextual Attention [58] takes a similar two-step approach. First, it produces a base estimate of the invisible region. Next, the refinement block sharpens the photo by background patch sets. The typical limitations of current face image generate schemes are the necessity of manipulation, the complexity of fundamental architectures, the degradation in accuracy, and the inability of restricting modification to local region.

## 3 Our Approach

### 3.1 Landmark Prediction Task

Fig.1 shows the entire process of our work. In the landmark prediction task, we found that generating accurate 68 feature points  $\mathbf{Z}_{\text{lmk}} \in \mathbb{R}^{2 \times 68}$  was a crucial

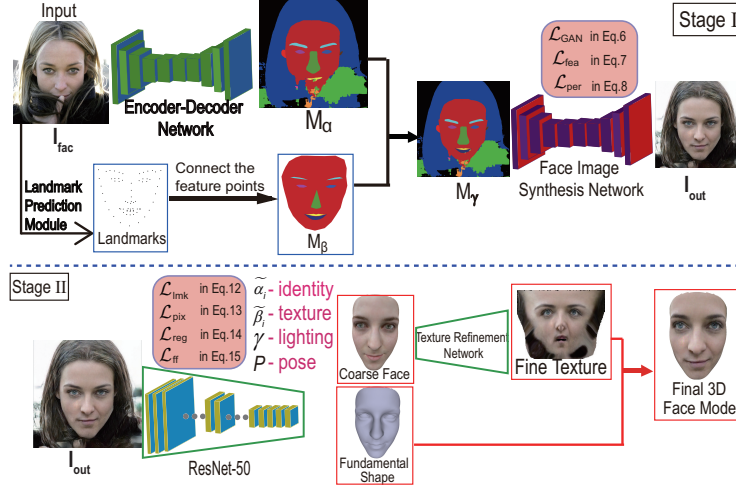


**Fig. 1.** Overall our pipeline. We first remove the occluded area and reconstruct the face with complete facial features. Then we utilize ResNet-50 and texture refinement network to reconstruct the final 3D model.

part under occlusion scenes. The architecture  $\mathcal{N}_{\text{lmk}}$  aims to generate landmarks from a corrupted face photo  $\mathbf{I}_{\text{cor}}$ :  $\mathbf{Z}_{\text{lmk}} = \mathcal{N}_{\text{lmk}}(\mathbf{I}_{\text{cor}}; \theta_{\text{lmk}})$ , where  $\theta_{\text{lmk}}$  denotes the trainable parameters. Since we want to focus more on efficiency and follow face parsing map generation task, we built a sufficiently effective  $\mathcal{N}_{\text{lmk}}$  upon the MobileNet-V3 [20].  $\mathcal{N}_{\text{lmk}}$  is focused on feature extraction, unlike traditional landmark detectors. The final module is realized by fully connecting the fused feature maps. We set the loss function  $\mathcal{L}_{\text{lmk}}$  as follows:

$$\mathcal{L}_{\text{lmk}} = \left\| \mathbf{Z}_{\text{lmk}}^{(i)} - \hat{\mathbf{Z}}_{\text{gt}}^{(i)} \right\|_2^2 \quad (1)$$

where  $\hat{\mathbf{Z}}_{\text{gt}}^{(i)}$  denotes the  $i$ th ground truth face landmarks.

### 3.2 Face Parsing Map Generation

Pixel-level recognition of occlusion and face skin areas is a prerequisite for our framework to ensure accuracy. To benefit from the annotated face dataset CelebAMask-HQ [29], we used an encoder-decoder architecture  $\mathcal{N}_{\alpha}$  based on U-Net [51] to estimate pixel-level label classes. Given a squarely resized face image  $\mathbf{I}_{\text{fac}} \in \mathbb{R}^{H \times W \times 3}$ , we applied the trained face parsing model  $\mathcal{N}_{\alpha}$  to obtain the parsing map  $\mathbf{M}_{\alpha} \in \mathbb{R}^{H \times W \times 1}$ . On the other hand, given the landmarks  $\mathbf{Z}_{\text{lmk}} \in \mathbb{R}^{2 \times 68}$ , we connected the feature points to form a region. Then these regions can form a parsing map  $\mathbf{M}_{\beta} \in \mathbb{R}^{H \times W \times 1}$  including facial features. Please notice that, in our work, we assumed that facial features only include only five parts, including facial skin, eyebrows, eyes, nose and lips. The final map  $\mathbf{M}_{\gamma} \in \mathbb{R}^{H \times W \times 1}$  (see Fig. 2) without occluded objects needs  $\mathbf{M}_{\alpha}$  plus  $\mathbf{M}_{\beta}$

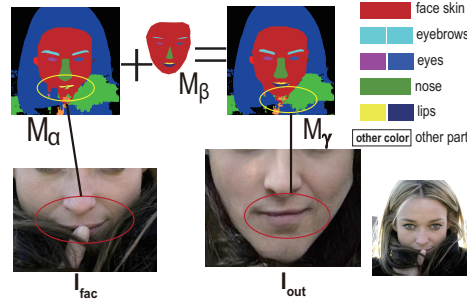


**Fig. 2.** Our face parsing map generation module, which follows Algorithm 1. The results shown in the figure show that our method finally successfully removed the occlusion of fingers and hair

. In order to generate  $M_\gamma$  including the complete facial features, we designed Algorithm 1.

**Algorithm 1** Face Parsing Map Plus Algorithm, our proposed algorithm. All experiments in the papers Map **A** and Map **B** have the same width and height.

**Input:**  $A_i$ , pixels point on the face parsing map **A**.  $B_i$ , pixels point on the face parsing map **B**.  $V(z)$ , the function of getting the grayscale value of point  $z$ .

$X(i)$ , the horizontal coordinate value of  $i$  in the map.  $Y(i)$ , the vertical coordinate value of  $i$  in the map.  $W$ , the width of the map.  $H$ , the height of the map.  $S$ , the gray value range of the facial features area (only include four parts:eyebrows, eyes, nose, lips).  $O$ , gray value range of the facial skin area.

**Input:** Face parsing map **A** and **B**

**Output:**  $C_i$ , pixels point on the new face parsing map **C**

```

1: while  $Y(i) \leq H$  do ▷ Start to generate complete face skin
2:   while  $X(i) \leq W$  do
3:     if  $A_i \in O$  then
4:        $C_i \leftarrow A_i, X(i) + 1 \leftarrow X(i)$ 
5:     else if  $A_i \text{ NOT } \in O \text{ AND } B_i \in O$  then
6:        $C_i \leftarrow B_i, X(i) + 1 \leftarrow X(i)$ 
7:     else  $C_i \leftarrow A_i, X(i) + 1 \leftarrow X(i)$ 
8:   end while
9:    $Y(i) + 1 \leftarrow Y(i)$ 
10: end while
11:
12: while  $Y(i) \leq H$  do ▷ Start to generate complete facial features
13:   while  $X(i) \leq W$  do
14:     if  $A_i \in S$  then
15:        $C_i \leftarrow A_i, X(i) + 1 \leftarrow X(i)$ 
16:     else if  $A_i \text{ NOT } \in S \text{ AND } B_i \in S$  then
17:        $C_i \leftarrow B_i, X(i) + 1 \leftarrow X(i)$ 
18:     else  $C_i \leftarrow A_i, X(i) + 1 \leftarrow X(i)$ 

```

```

19:         end while
20:     Y(i) + 1 ← Y(i)
21: end while

```

---

### 3.3 Face Image Synthesis with GAN

**Face Image Synthesis Network** To benefit from the Pix2Pix architecture, we proposed a Face Image Synthesis Network (FISN)  $\mathcal{N}_{et}$ , which was based on Pix2PixHD [65] as a backbone. FISN receives  $\mathbf{I}_{fac} \in \mathbb{R}^{H \times W \times 3}$  and  $\mathbf{M}_{\alpha}$  as inputs. The detailed architecture is shown in Fig.1. To fuse  $\mathbf{I}_{fac}$  and  $\mathbf{M}_{\alpha}$ , we used Spatial Feature Transform (SFT) layer [44] learned a mapping function  $\mathcal{M}$  that outputs a parameter pair  $(\gamma, \beta)$  based on the prior condition  $\Psi$  from the features  $\mathbf{M}_{\alpha}$ . A pair of affine transformation parameters  $(\gamma, \beta)$  model the prior  $\Psi$ . Here, the mapping equation can be expressed as  $(\gamma, \beta) = M(\Psi)$ . After obtaining  $(\gamma, \beta)$ , the transformation is carried out by the SFT layer:

$$SFT(\mathbf{F}_{map} | \gamma, \beta) = \gamma \odot F + \beta \quad (2)$$

where  $\mathbf{F}_{map}$  denotes the feature maps from  $\mathbf{I}_{fac}$ ,  $\odot$  denotes Hadamard product. Therefore, we conditioned spatial information  $\mathbf{M}_{\alpha}$  on style data  $\mathbf{I}_{fac}$  and generated affine parameters  $(x_i, y_i)$  followed  $(x_i, y_i) = \mathcal{N}_{et}(I_{fac}, M_{\alpha})$ . Related research [44] showed that ordinary normalization layers would "wash away" semantic information. To transfer  $(x_i, y_i)$  to new mask input  $\mathbf{M}_{\gamma}$ , we utilized semantic region-adaptive normalization (SEAN) [75] on residual blocks  $z_i$  in the FISN. Let  $H$ ,  $W$  and  $C$  be the height, width and the number of channels in the activation map of the deep convolutional network for a batch of  $N$  samples. The modulated activation value at the site was defined as:

$$SEAN(z_i, x_i, y_i) = x_i \frac{z_i - \mu(z_i)}{\sigma(z_i)} + y_i \quad (3)$$

where  $\mu(z_i)$  and  $\sigma(z_i)$  are the mean and standard deviation of the activation  $(n \in N, c \in C, y \in H, x \in W)$  in channel  $c$ :

$$\mu(z_i) = \frac{1}{NHW} \sum_{n,y,x} h_{n,c,y,x} \quad (4)$$

$$\sigma(z_i) = \sqrt{\frac{1}{NHW} \sum_{n,y,x} \left( (h_{n,c,y,x})^2 - \mu(z_i)^2 \right)} \quad (5)$$

FISN is a generator that learns the style mapping between  $\mathbf{I}_{fac}$  and  $\mathbf{M}_{\gamma}$  according to the spatial information provided by  $\mathbf{M}_{\alpha}$ . Therefore, face features (*e.g.* eyes style) in  $\mathbf{I}_{fac}$  are shifted to the corresponding position on  $\mathbf{M}_{\gamma}$  so that FISN can synthesis image  $\mathbf{I}_{out}$  which removed occlusion.

**Loss Function** The design of our loss function for FISN is inspired by Pix2PixHD [65], MaskGAN [29] and SEAN [75], which contains three components:

(1) *Adversarial loss*. Let  $D_1$  and  $D_2$  be two discriminators at different scales,  $\mathcal{L}_{GAN}$  is the conditional adversarial loss defined by

$$\mathcal{L}_{GAN} = \mathbb{E} [\log (D_{1,2}(\mathbf{I}_{\text{fac}}, \mathbf{M}_{\alpha}))] + \mathbb{E} [1 - \log (D_{1,2}(\mathbf{I}_{\text{out}}, \mathbf{M}_{\alpha}))] \quad (6)$$

(2) *Feature matching loss* [65]. Let  $T$  be the total number of layers in discriminator  $D$ .  $\mathcal{L}_{\text{fea}}$  is the feature matching loss which computed the  $L_1$  distance between the real and generated face image defined by

$$\mathcal{L}_{\text{fea}} = \mathbb{E} \sum_{i=1}^T \left\| D_{1,2}^{(i)}(\mathbf{I}_{\text{fac}}, \mathbf{M}_{\alpha}) - D_{1,2}^{(i)}(\mathbf{I}_{\text{out}}, \mathbf{M}_{\alpha}) \right\|_1 \quad (7)$$

(3) *Perceptual loss* [25]. Let  $N$  be the total number of layers used to calculate the perceptual loss,  $F^{(i)}$  be the output feature maps of the  $i$ th layer of the VGG network [56].  $\mathcal{L}_{\text{per}}$  is the perceptual loss which computes the  $L_1$  distance between the real and generated face image defined by

$$\mathcal{L}_{\text{per}} = \mathbb{E} \sum_{i=1}^N \frac{1}{M_i} \left[ \left\| F^{(i)}(\mathbf{I}_{\text{fac}}) - F^{(i)}(\mathbf{I}_{\text{out}}) \right\|_1 \right] \quad (8)$$

The final loss function of FISN used in our experiment is made up of the above-mentioned three loss terms as:

$$\mathcal{L}_{FISN} = \mathcal{L}_{GAN} + \lambda_1 \mathcal{L}_{\text{fea}} + \lambda_2 \mathcal{L}_{\text{per}} \quad (9)$$

where we set  $\lambda_1 = \lambda_2 = 10$  respectively in our experiments.

### 3.4 Camera and Illumination Model

Given an face image, we adopt the Basel Face Model (BFM) [47]. After the 3D face is reconstructed, it can be projected onto the image plane with the perspective projection:

$$V_{2d}(\mathbf{P}) = f * \mathbf{P}_r * \mathbf{R} * \mathbf{S}_{\text{mod}} + \mathbf{t}_{2d} \quad (10)$$

where  $V_{2d}(\mathbf{P})$  denotes the projection function that turned the 3D model into 2D face positions,  $f$  denotes the scale factor,  $\mathbf{P}_r$  denotes the projection matrix,  $\mathbf{R} \in SO(3)$  denotes the rotation matrix,  $\mathbf{S}_{\text{mod}}$  denotes the shape of the face and  $\mathbf{t}_{2d} \in \mathbb{R}^3$  denotes the translation vector.

We approximated the scene illumination with Spherical Harmonics (SH) [11] for face. Thus, we can compute the face as Lambertian surface and skin texture follows:

$$\mathbf{C}(\mathbf{r}_i, \mathbf{n}_i, \gamma) = \mathbf{r}_i \odot \sum_{b=1}^{B^2} \gamma_b \Phi_b(\mathbf{n}_i) \quad (11)$$

where  $\mathbf{r}_i$  denotes skin reflectance,  $\mathbf{n}_i$  denotes surface normal,  $\odot$  denotes the Hadamard product,  $\gamma \in \mathbb{R}^9$  under monochromatic lights condition,  $\Phi_b : \mathbb{R}^3 \rightarrow \mathbb{R}$  denotes SH basis function,  $B$  denotes the number of spherical harmonics bands and  $\gamma_{\mathbf{b}} \in \mathbb{R}^3$  (here we set  $B = 3$ ) denotes the corresponding SH coefficients.

Therefore, parameters to be learned can be denoted by a vector  $\mathbf{y} = (\widetilde{\alpha}_i, \widetilde{\beta}_i, \gamma, \mathbf{p}) \in \mathbb{R}^{175}$ , where  $\mathbf{p} \in \mathbb{R}^6 = \{\textit{pitch}, \textit{yaw}, \textit{roll}, \textit{f}, \textit{t}_{2D}\}$  denotes face poses. In this work, we used a fixed ResNet-50 [18] network to regress these coefficients. The loss function of ResNet-50 follows Eq.16. We then got the fundamental shape  $\mathbf{S}_{\text{base}}$  (coordinate, e.g.  $x, y, z$ ) and the coarse texture  $\mathbf{T}_{\text{coa}}$  (albedo, e.g.  $r, g, b$ ). We used a coarse-to-fine network based on graph convolutional networks of Lin *et al.* [32] for producing the fine texture  $\mathbf{T}_{\text{fin}}$ .

### 3.5 Loss Function of 3D Reconstruction

Given a generated image  $\mathbf{I}_{\text{out}}$ , we used the ResNet to regress the corresponding coefficient  $y$ . The design of loss function for ResNet contained four components: (1) Landmark Loss. As facial landmarks convey the structural information of the human face, we used landmark loss to measure how close projected shape landmark vertices to the corresponding landmarks in the image  $\mathbf{I}_{\text{out}}$ . We ran the landmark prediction module  $\mathcal{N}_{lmk}$  to detect 68 landmarks  $\{z_{lmk}^{(n)}\}$  from the training images. We obtained landmarks  $\{l_y^{(n)}\}$  from rendering facial images. Then, we computed the loss as:

$$\mathcal{L}_{lmk}(y) = \frac{1}{N} \sum_{n=1}^N \left\| z_{lmk}^{(n)} - l_y^{(n)} \right\|_2^2 \quad (12)$$

where  $\|\cdot\|_2$  denotes the  $L_2$  norm.

(2) Accurate Pixel-wise Loss. The rendering layer renders back an image  $\mathbf{I}_y^{(i)}$  to compare with the image  $\mathbf{I}_{\text{out}}^{(i)}$ . The pixel-wise loss is formulated as:

$$\mathcal{L}_{\text{pix}}(y) = \frac{\sum_{i \in \mathcal{M}} P_i \cdot \left\| \mathbf{I}_{\text{out}}^{(i)} - \mathbf{I}_y^{(i)} \right\|_2}{\sum_{i \in \mathcal{M}} P_i} \quad (13)$$

where  $i$  denotes pixel index,  $\mathcal{M}$  is the reprojected face region which obtained with landmarks [42],  $\|\cdot\|_2$  denotes the  $L_2$  norm and  $P_i$  is occlusion attention coefficient which is described as follows. To gain robustness to accurate texture, we set  $P_i = \begin{cases} 1 & \text{if } i \in \text{facial features of } M_\alpha \\ 0.1 & \text{otherwise} \end{cases}$  for each pixel  $i$ .

(3) Regularization Loss. To prevent shape deformation and texture degeneration, we introduce the prior distribution to the parameters of the face model. We add the regularization loss as:

$$\mathcal{L}_{\text{reg}} = \omega_\alpha \|\widetilde{\alpha}_i\|^2 + \omega_\beta \|\widetilde{\beta}_i\|^2 \quad (14)$$



here, we set  $\omega_\alpha=1.0, \omega_\beta = 1.75e-3$  respectively.

(4)Face Features Level Loss. To reduce the difference between 3D face with 2D image, we define the loss at face recognition level. The loss computes the feature difference between the input image  $\mathbf{I}_{out}$  and rendered image  $\mathbf{I}_y$ . We define the loss as a cosine distance:

$$\mathcal{L}_{ff}=1-\frac{\langle G(\mathbf{I}_{out}), G(\mathbf{I}_y) \rangle}{\|G(\mathbf{I}_{out})\| \cdot \|G(\mathbf{I}_y)\|} \quad (15)$$

where  $G(\cdot)$  denotes the feature extraction function by FaceNet [53],  $\langle \cdot, \cdot \rangle$  denotes the inner product.

In summary, the final loss function of 3D face reconstruction used in our experiment is made up of the above-mentioned four loss terms as:

$$\mathcal{L}_{3D}=\lambda_3\mathcal{L}_{lmk} + \lambda_4\mathcal{L}_{pix} + \lambda_5\mathcal{L}_{reg} + \lambda_6\mathcal{L}_{ff} \quad (16)$$

where we set  $\lambda_3= 1.6e - 3, \lambda_4= 1.4, \lambda_5= 3.7e-4, \lambda_6= 0.2$  respectively in all our experiments.

## 4 Implementation Details

Considering the question of landmark predictor, the 300-W dataset [52] has labeled ground truth landmarks, while the CelebA-HQ dataset [27] does not. We generated the ground truth of CelebA-HQ by the Faceboxes predictor [71] as the reference. In experiments shown in this work, we use the  $256 \times 256$  images for training the landmark predictor  $\mathcal{N}_{lmk}$  and the batch size= 16. The learning rate of  $\mathcal{N}_{lmk}$  is  $10e - 4$ . We use the trained face parsing model  $\mathcal{N}_\alpha$  [29] to generate  $\mathbf{M}_\alpha$ . We obtain  $\mathbf{M}_\gamma$  according to Algorithm 1. FISN follows the design of Pix2PixHD [65] with four residual blocks. To train the FISN, we used the CelebAMask-HQ dataset which has 30000 semantic labels with a size of  $512 \times 512$ . Each label clearly marked the facial features of the face.

FISN does not use any ordinary normalization layers (*e.g.* Instance Normalization) which will wash away style information. Before training the ResNet, we take the weights from pre-trained of R-Net [11] as initialization. We set the input image size to  $224 \times 224$  and the number of vertices to 35709. We design our texture refinement network based on the Graph Convolutional Network method of Lin *et al.* [32]. We do not adopt any fully-connected layers or convolutional layers in the refinement network refer to related research [32]. This will reduce the performance of the module.

## 5 Experimental Results

### 5.1 Qualitative Comparisons with Recent Works

Fig.3 shows our results compared with the other work. The last two columns show our results. The remaining columns demonstrate the results of 3DDFA [17],

DF<sup>2</sup>Net [70] and Chen *et al.* [3]. Qualitative results show that our method surpasses other methods. Fig.3 shows that our method can reconstruct a complete face model under occlusion scenes such as glasses, jewelry, palms, and hair. Other methods focused on generating high-resolution face textures. These frameworks cannot effectively deal with occluded scenes.

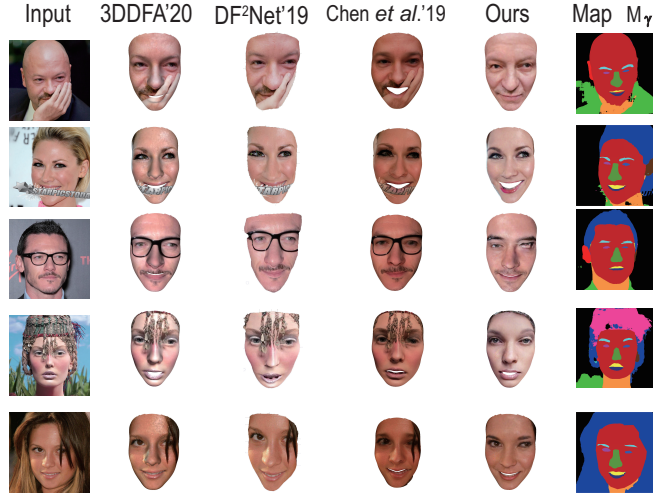


**Fig. 3.** Comparison of qualitative results. Baseline methods from left to right: 3DDFA, DF<sup>2</sup>Net, Chen *et al.* and our method.

## 5.2 Quantitative Comparison

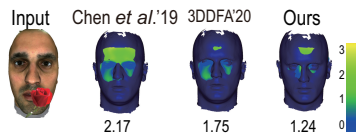


**Fig. 4.** Comparison of error heat maps on the MICC Florence datasets. Digits denote 90% error (mm).

**Comparison result on the MICC Florence datasets** MICC Florence dataset [2] is a 3D face dataset that contains 53 faces with their ground truth models. We artificially added some occluders as input. We calculated the average 90% largest error between the generative model and the ground truth model. Fig.4 shows that our method can effectively handle occlusion.

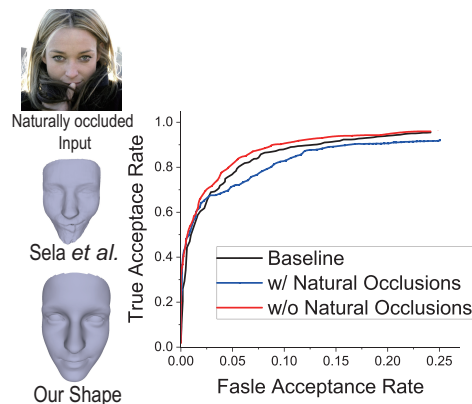


**Fig. 5.** Reconstructions with occlusions. Left: Qualitative results of Sela *et al.* [54] and our shape. Right: LFW verification ROC for the shapes, with and without occlusions.

**Occlusion invariance of the foundation shape** Our choice of using the ResNet-50 to regress the shape coefficients is motivated by the unique robustness to extreme viewing conditions in the paper of Deng *et al.* [11]. To fully support the application of our method to occluded face images, we test our system on the Labeled Faces in the Wild datasets (LFW) [21]. We used the same face test system from Anh *et al.* [62], and we refer to that paper for more details. Fig. 5 (left) shows the sensitivity of the method of Sela *et al.* [54]. Their result clearly shows the outline of a finger. Their failure may be due to more focus on local details, which weakly regularizes the global shape. However, our method recognizes and regenerates the occluded area. Our method much robust provides a natural face shape under common occlusion scenes. Though 3DMM also limits the details of shape, we use it only as a foundation and add refined texture separately.

**Table 1.** Quantitative evaluations on LFW.

Method	100%-EER	Accuracy	nAUC
Tran <i>et al.</i> [61]	$89.40 \pm 1.52$	$89.36 \pm 1.25$	$95.90 \pm 0.95$
Ours (w/ Occ)	$85.75 \pm 1.12$	$86.49 \pm 0.97$	$93.89 \pm 1.31$
Ours (w/o Occ)	$90.57 \pm 1.43$	$89.87 \pm 0.71$	$96.59 \pm 0.37$

We further quantitatively verify the robustness of our method to occlusions. Table 1 (top) reports verification results on the LFW benchmark with and without occlusions (see also ROC in Fig.5 (right)). Though occlusions clearly impact recognition, this drop of the curve is limited, demonstrating the robustness of our method.

## 6 Conclusions

In this work, we present a novel single-image 3D face reconstruction method under occluded scenes with high fidelity textures. Comprehensive experiments have shown that our method outperforms previous methods by a large margin in terms of both accuracy and robustness. Future work includes combining our method with Transformer architecture to further improve accuracy.

## 7 Acknowledgment

This paper is supported by National Natural Science Foundation of China (No. 62072020), National Key Research and Development Program of China (No. 2017YFB1002602), Key-Area Research and Development Program of Guangdong Province (No. 2019B010150001) and the Leading Talents in Innovation and Entrepreneurship of Qingdao (19-3-2-21-zhc).

## Bibliography

- [1] Abdal, R., Qin, Y., Wonka, P.: Image2stylegan: How to embed images into the stylegan latent space? In: Proceedings of the IEEE/CVF International Conference on Computer Vision. pp. 4432–4441 (2019)
- [2] Bagdanov, A.D., Del Bimbo, A., Masi, I.: The florence 2d/3d hybrid face dataset. In: Proceedings of the 2011 joint ACM workshop on Human gesture and behavior understanding. pp. 79–80 (2011)
- [3] Chen, A., Chen, Z., Zhang, G., Mitchell, K., Yu, J.: Photo-realistic facial details synthesis from single image. In: Proceedings of the IEEE International Conference on Computer Vision. pp. 9429–9439 (2019)
- [4] Chen, L.C., Papandreou, G., Kokkinos, I., Murphy, K., Yuille, A.L.: Semantic image segmentation with deep convolutional nets and fully connected crfs. arXiv preprint arXiv:1412.7062 (2014)
- [5] Chen, L.C., Papandreou, G., Kokkinos, I., Murphy, K., Yuille, A.L.: Deeplab: Semantic image segmentation with deep convolutional nets, atrous convolution, and fully connected crfs. *IEEE transactions on pattern analysis and machine intelligence* **40**(4), 834–848 (2017)
- [6] Chen, L.C., Papandreou, G., Schroff, F., Adam, H.: Rethinking atrous convolution for semantic image segmentation. arXiv preprint arXiv:1706.05587 (2017)
- [7] Chen, L.C., Zhu, Y., Papandreou, G., Schroff, F., Adam, H.: Encoder-decoder with atrous separable convolution for semantic image segmentation. In: Proceedings of the European conference on computer vision (ECCV). pp. 801–818 (2018)
- [8] Choi, Y., Choi, M., Kim, M., Ha, J.W., Kim, S., Choo, J.: Stargan: Unified generative adversarial networks for multi-domain image-to-image translation. In: Proceedings of the IEEE Conference on Computer Vision and Pattern Recognition. pp. 8789–8797 (2018)
- [9] Chu, W., Hung, W.C., Tsai, Y.H., Cai, D., Yang, M.H.: Weakly-supervised caricature face parsing through domain adaptation. In: 2019 IEEE International Conference on Image Processing (ICIP). pp. 3282–3286. IEEE (2019)
- [10] Demir, U., Unal, G.: Patch-based image inpainting with generative adversarial networks. arXiv preprint arXiv:1803.07422 (2018)
- [11] Deng, Y., Yang, J., Xu, S., Chen, D., Jia, Y., Tong, X.: Accurate 3d face reconstruction with weakly-supervised learning: From single image to image set. In: Proceedings of the IEEE Conference on Computer Vision and Pattern Recognition Workshops. pp. 0–0 (2019)
- [12] Dolhansky, B., Ferrer, C.C.: Eye in-painting with exemplar generative adversarial networks. In: Proceedings of the IEEE conference on computer vision and pattern recognition. pp. 7902–7911 (2018)
- [13] Dumoulin, V., Shlens, J., Kudlur, M.: A learned representation for artistic style. arXiv preprint arXiv:1610.07629 (2016)

- [14] Feng, Y., Wu, F., Shao, X., Wang, Y., Zhou, X.: Joint 3d face reconstruction and dense alignment with position map regression network. In: Proceedings of the European Conference on Computer Vision (ECCV). pp. 534–551 (2018)
- [15] Frühstück, A., Alhashim, I., Wonka, P.: Tilegan: synthesis of large-scale non-homogeneous textures. *ACM Transactions on Graphics (TOG)* **38**(4), 1–11 (2019)
- [16] Goodfellow, I.J., Pouget-Abadie, J., Mirza, M., Xu, B., Warde-Farley, D., Ozair, S., Courville, A., Bengio, Y.: Generative adversarial networks. *arXiv preprint arXiv:1406.2661* (2014)
- [17] Guo, J., Zhu, X., Yang, Y., Yang, F., Lei, Z., Li, S.Z.: Towards fast, accurate and stable 3d dense face alignment. *arXiv preprint arXiv:2009.09960* (2020)
- [18] He, K., Zhang, X., Ren, S., Sun, J.: Deep residual learning for image recognition. In: Proceedings of the IEEE conference on computer vision and pattern recognition. pp. 770–778 (2016)
- [19] He, Z., Zuo, W., Kan, M., Shan, S., Chen, X.: Attgan: Facial attribute editing by only changing what you want. *arXiv preprint arXiv:1711.10678* (2017)
- [20] Howard, A., Sandler, M., Chu, G., Chen, L.C., Chen, B., Tan, M., Wang, W., Zhu, Y., Pang, R., Vasudevan, V.: Searching for mobilenetv3. In: Proceedings of the IEEE/CVF International Conference on Computer Vision. pp. 1314–1324 (2019)
- [21] Huang, G.B., Mattar, M., Berg, T., Learned-Miller, E.: Labeled faces in the wild: A database for studying face recognition in unconstrained environments. In: Workshop on faces in 'Real-Life' Images: detection, alignment, and recognition (2008)
- [22] Huang, X., Belongie, S.: Arbitrary style transfer in real-time with adaptive instance normalization. In: Proceedings of the IEEE International Conference on Computer Vision. pp. 1501–1510 (2017)
- [23] Isola, P., Zhu, J.Y., Zhou, T., Efros, A.A.: Image-to-image translation with conditional adversarial networks. In: Proceedings of the IEEE conference on computer vision and pattern recognition. pp. 1125–1134 (2017)
- [24] Jaderberg, M., Simonyan, K., Zisserman, A., Kavukcuoglu, K.: Spatial transformer networks. *arXiv preprint arXiv:1506.02025* (2015)
- [25] Johnson, J., Alahi, A., Fei-Fei, L.: Perceptual losses for real-time style transfer and super-resolution. In: European conference on computer vision. pp. 694–711. Springer (2016)
- [26] Jourabloo, A., Liu, X.: Large-pose face alignment via cnn-based dense 3d model fitting. In: Proceedings of the IEEE conference on computer vision and pattern recognition. pp. 4188–4196 (2016)
- [27] Karras, T., Aila, T., Laine, S., Lehtinen, J.: Progressive growing of gans for improved quality, stability, and variation. *arXiv preprint arXiv:1710.10196* (2017)
- [28] Karras, T., Laine, S., Aittala, M., Hellsten, J., Lehtinen, J., Aila, T.: Analyzing and improving the image quality of stylegan. In: Proceedings of the IEEE/CVF Conference on Computer Vision and Pattern Recognition. pp. 8110–8119 (2020)

- [29] Lee, C.H., Liu, Z., Wu, L., Luo, P.: Maskgan: Towards diverse and interactive facial image manipulation. In: Proceedings of the IEEE/CVF Conference on Computer Vision and Pattern Recognition. pp. 5549–5558 (2020)
- [30] Li, C., Wand, M.: Precomputed real-time texture synthesis with markovian generative adversarial networks. In: European conference on computer vision. pp. 702–716. Springer (2016)
- [31] Li, M., Zuo, W., Zhang, D.: Deep identity-aware transfer of facial attributes. arXiv preprint arXiv:1610.05586 (2016)
- [32] Lin, J., Yuan, Y., Shao, T., Zhou, K.: Towards high-fidelity 3d face reconstruction from in-the-wild images using graph convolutional networks. arXiv preprint arXiv:2003.05653 (2020)
- [33] Lin, J., Yang, H., Chen, D., Zeng, M., Wen, F., Yuan, L.: Face parsing with roi tanh-warping. In: Proceedings of the IEEE Conference on Computer Vision and Pattern Recognition. pp. 5654–5663 (2019)
- [34] Lin, Y., Shen, J., Wang, Y., Pantic, M.: Roi tanh-polar transformer network for face parsing in the wild. *Image and Vision Computing* p. 104190 (2021)
- [35] Liu, F., Zeng, D., Zhao, Q., Liu, X.: Joint face alignment and 3d face reconstruction. In: European Conference on Computer Vision. pp. 545–560. Springer (2016)
- [36] Liu, M.Y., Breuel, T., Kautz, J.: Unsupervised image-to-image translation networks. arXiv preprint arXiv:1703.00848 (2017)
- [37] Liu, Z., Luo, P., Wang, X., Tang, X.: Deep learning face attributes in the wild. In: Proceedings of the IEEE international conference on computer vision. pp. 3730–3738 (2015)
- [38] Long, J., Shelhamer, E., Darrell, T.: Fully convolutional networks for semantic segmentation. In: Proceedings of the IEEE conference on computer vision and pattern recognition. pp. 3431–3440 (2015)
- [39] Mirza, M., Osindero, S.: Conditional generative adversarial nets. arXiv preprint arXiv:1411.1784 (2014)
- [40] Miyato, T., Kataoka, T., Koyama, M., Yoshida, Y.: Spectral normalization for generative adversarial networks. arXiv preprint arXiv:1802.05957 (2018)
- [41] Nazeri, K., Ng, E., Joseph, T., Qureshi, F.Z., Ebrahimi, M.: Edgeconnect: Generative image inpainting with adversarial edge learning. arXiv preprint arXiv:1901.00212 (2019)
- [42] Nirkin, Y., Masi, I., Tuan, A.T., Hassner, T., Medioni, G.: On face segmentation, face swapping, and face perception. In: 2018 13th IEEE International Conference on Automatic Face & Gesture Recognition (FG 2018). pp. 98–105. IEEE (2018)
- [43] Pan, J., Wang, C., Jia, X., Shao, J., Sheng, L., Yan, J., Wang, X.: Video generation from single semantic label map. In: Proceedings of the IEEE/CVF Conference on Computer Vision and Pattern Recognition. pp. 3733–3742 (2019)
- [44] Park, T., Liu, M.Y., Wang, T.C., Zhu, J.Y.: Semantic image synthesis with spatially-adaptive normalization. In: Proceedings of the IEEE Conference on Computer Vision and Pattern Recognition. pp. 2337–2346 (2019)
- [45] Parkhi, O.M., Vedaldi, A., Zisserman, A.: Deep face recognition (2015)

- [46] Pathak, D., Krahenbuhl, P., Donahue, J., Darrell, T., Efros, A.A.: Context encoders: Feature learning by inpainting. In: Proceedings of the IEEE conference on computer vision and pattern recognition. pp. 2536–2544 (2016)
- [47] Paysan, P., Knothe, R., Amberg, B., Romdhani, S., Vetter, T.: A 3d face model for pose and illumination invariant face recognition. In: 2009 Sixth IEEE International Conference on Advanced Video and Signal Based Surveillance. pp. 296–301. Ieee (2009)
- [48] Pizzati, F., Cerri, P., de Charette, R.: Comogan: continuous model-guided image-to-image translation. arXiv preprint arXiv:2103.06879 (2021)
- [49] Richardson, E., Sela, M., Kimmel, R.: 3d face reconstruction by learning from synthetic data. In: 2016 Fourth International Conference on 3D Vision (3DV). pp. 460–469. IEEE (2016)
- [50] Richardson, E., Sela, M., Or-El, R., Kimmel, R.: Learning detailed face reconstruction from a single image. In: Proceedings of the IEEE Conference on Computer Vision and Pattern Recognition. pp. 1259–1268 (2017)
- [51] Ronneberger, O., Fischer, P., Brox, T.: U-net: Convolutional networks for biomedical image segmentation. In: International Conference on Medical image computing and computer-assisted intervention. pp. 234–241. Springer (2015)
- [52] Sagonas, C., Tzimiropoulos, G., Zafeiriou, S., Pantic, M.: 300 faces in-the-wild challenge: The first facial landmark localization challenge. In: Proceedings of the IEEE International Conference on Computer Vision Workshops. pp. 397–403 (2013)
- [53] Schroff, F., Kalenichenko, D., Philbin, J.: Facenet: A unified embedding for face recognition and clustering. In: Proceedings of the IEEE conference on computer vision and pattern recognition. pp. 815–823 (2015)
- [54] Sela, M., Richardson, E., Kimmel, R.: Unrestricted facial geometry reconstruction using image-to-image translation. In: Proceedings of the IEEE International Conference on Computer Vision. pp. 1576–1585 (2017)
- [55] Shen, W., Liu, R.: Learning residual images for face attribute manipulation. In: Proceedings of the IEEE conference on computer vision and pattern recognition. pp. 4030–4038 (2017)
- [56] Simonyan, K., Zisserman, A.: Very deep convolutional networks for large-scale image recognition. arXiv preprint arXiv:1409.1556 (2014)
- [57] Slossberg, R., Shamaï, G., Kimmel, R.: High quality facial surface and texture synthesis via generative adversarial networks. In: Proceedings of the European Conference on Computer Vision (ECCV) Workshops. pp. 0–0 (2018)
- [58] Song, Y., Yang, C., Lin, Z., Liu, X., Huang, Q., Li, H., Kuo, C.C.J.: Contextual-based image inpainting: Infer, match, and translate. In: Proceedings of the European Conference on Computer Vision (ECCV). pp. 3–19 (2018)
- [59] Strudel, R., Garcia, R., Laptev, I., Schmid, C.: Segmenter: Transformer for semantic segmentation. arXiv preprint arXiv:2105.05633 (2021)
- [60] Tripathi, S., Bhiwandiwala, A., Bastidas, A., Tang, H.: Heuristics for image generation from scene graphs (2019)



- [61] Tuan Tran, A., Hassner, T., Masi, I., Medioni, G.: Regressing robust and discriminative 3d morphable models with a very deep neural network. In: Proceedings of the IEEE Conference on Computer Vision and Pattern Recognition. pp. 5163–5172 (2017)
- [62] Tuan Tran, A., Hassner, T., Masi, I., Paz, E., Nirkin, Y., Medioni, G.: Extreme 3d face reconstruction: Seeing through occlusions. In: Proceedings of the IEEE Conference on Computer Vision and Pattern Recognition. pp. 3935–3944 (2018)
- [63] Ulyanov, D., Vedaldi, A., Lempitsky, V.: Instance normalization: The missing ingredient for fast stylization. arXiv preprint arXiv:1607.08022 (2016)
- [64] Wang, S., Cheng, Z., Deng, X., Chang, L., Duan, F., Lu, K.: Leveraging 3d blendshape for facial expression recognition using cnn. *Sci. China Inf. Sci* **63**(120114), 1–120114 (2020)
- [65] Wang, T.C., Liu, M.Y., Zhu, J.Y., Tao, A., Kautz, J., Catanzaro, B.: High-resolution image synthesis and semantic manipulation with conditional gans. In: Proceedings of the IEEE conference on computer vision and pattern recognition. pp. 8798–8807 (2018)
- [66] Wei, Z., Sun, Y., Wang, J., Lai, H., Liu, S.: Learning adaptive receptive fields for deep image parsing network. In: Proceedings of the IEEE conference on computer vision and pattern recognition. pp. 2434–2442 (2017)
- [67] Xiao, T., Hong, J., Ma, J.: Elegant: Exchanging latent encodings with gan for transferring multiple face attributes. In: Proceedings of the European conference on computer vision (ECCV). pp. 168–184 (2018)
- [68] Yin, Z., Yiu, V., Hu, X., Tang, L.: End-to-end face parsing via interlinked convolutional neural networks. *Cognitive Neurodynamics* **15**(1), 169–179 (2021)
- [69] Yu, J., Lin, Z., Yang, J., Shen, X., Lu, X., Huang, T.S.: Generative image inpainting with contextual attention. In: Proceedings of the IEEE conference on computer vision and pattern recognition. pp. 5505–5514 (2018)
- [70] Zeng, X., Peng, X., Qiao, Y.: Df2net: A dense-fine-finer network for detailed 3d face reconstruction. In: Proceedings of the IEEE International Conference on Computer Vision. pp. 2315–2324 (2019)
- [71] Zhang, S., Zhu, X., Lei, Z., Shi, H., Wang, X., Li, S.Z.: Faceboxes: A cpu real-time face detector with high accuracy. In: 2017 IEEE International Joint Conference on Biometrics (IJCB). pp. 1–9. IEEE (2017)
- [72] Zhou, L., Liu, Z., He, X.: Face parsing via a fully-convolutional continuous crf neural network. arXiv preprint arXiv:1708.03736 (2017)
- [73] Zhu, J.Y., Krähenbühl, P., Shechtman, E., Efros, A.A.: Generative visual manipulation on the natural image manifold. In: European conference on computer vision. pp. 597–613. Springer (2016)
- [74] Zhu, J.Y., Park, T., Isola, P., Efros, A.A.: Unpaired image-to-image translation using cycle-consistent adversarial networks. In: Proceedings of the IEEE international conference on computer vision. pp. 2223–2232 (2017)
- [75] Zhu, P., Abdal, R., Qin, Y., Wonka, P.: Sean: Image synthesis with semantic region-adaptive normalization. In: Proceedings of the IEEE/CVF Conference on Computer Vision and Pattern Recognition. pp. 5104–5113 (2020)

- [76] Zhu, X., Lei, Z., Liu, X., Shi, H., Li, S.Z.: Face alignment across large poses: A 3d solution. In: Proceedings of the IEEE conference on computer vision and pattern recognition. pp. 146–155 (2016)